Hydrophilic Conjugated Polymers for Sustainable Fabrication of Deep-Red Light-Emitting Electrochemical Cells

ADVANCED MATERIALS TECHNOLOGIES
www.advmattechnol.de

Hydrophilic Conjugated Polymers for Sustainable Fabrication of Deep-Red Light-Emitting Electrochemical Cells

Tadele T. Filate, Shi Tang, Zewdneh Genene, Ludvig Edman, Wendimagegn Mammo,* and Ergang Wang**

It is crucial to develop functional electronic materials that can be processed from green solvents to achieve environmentally sustainable and cost-efficient printing fabrication of organic electronic devices. Here, the design and cost-efficient synthesis of two hydrophilic and emissive conjugated polymers, TQ-OEG and TQ2F-OEG, are presented, which are rendered hydrophilic through the grafting of oligo(ethylene glycol) (OEG) solubilizing groups onto the thiophene-quinoxaline conjugated backbone and thereby can be processed from a water:ethanol solvent mixture. It is shown that the introduction of the OEG groups enables for a direct dissolution of salts by the neat polymer for the attainment of solid-state ion mobility. These properties are utilized for the design and development of light-emitting electrochemical cells (LECs), the active materials of which can be solution cast from a water:ethanol-based ink. It is specifically shown that such an LEC device, comprising an optimized blend of the TQ2F-OEG emitter and a Li salt as the active material positioned between two air-stabile electrodes, delivers deep-red emission (peak wavelength = 670 nm) with a radiance of 185 μW m^{-2} at a low drive voltage of 2.3 V. This study contributes relevant information as to how polymers and LEC devices can be designed and fabricated to combine functionality with sustainability.

1. Introduction

Conjugated polymers attract attention for a large number of light-harvesting, energy-storage, sensing, and luminescent applications,[1] in significant part because they can enable low-cost solution-based device fabrication.[2] Hitherto, intense research has resulted in an impressive improvement of the device performance, but an unfortunate fact is that non-sustainable halogenated and/or aromatic liquids remain the common choice for the processing solvents. The use of such solvents poses serious health, environmental, and safety hazards, and it is thus timely to develop organic semiconductors that can be processed from more sustainable solvents.

In this context, Edman and coworkers[3] recently presented a green solvent selection tool, which utilizes the Hansen solubility parameters, in combination with well-established sustainability predictors, for the rational identification of ecofriendly replacement solvents. It should further be noted that a complete lifecycle analysis of a solvent should not only concern its environmental, safety, and health impacts during use, but also consider its synthesis. The latter is particularly true for non-recycled solvents that are synthesized from exhaustible fossil compounds. The fermentation of abundant and replenishable sugar-, starch- and lignocellulose-containing materials for the synthesis of ethanol addresses this issue.[4] Therefore, pure ethanol, water, and a mixture of ethanol and water can be ideal solvents with an attractive combination of suppressed health hazards and low ecological footprint during both synthesis and usage.[4b,5] However, the use of water as a solvent should be exercised with caution, particularly during recycling, since it otherwise can result in contamination of critical water resources.[6]

Most conjugated polymers exhibit a hydrophobic chemical structure, and they therefore exhibit poor or no solubility in polar solvents, such as alcohols and water.[7] Structural modification is thus crucial to render conjugated polymers soluble in polar and more ecofriendly solvents. Previous work in this direction has focused on either endowing the conjugated polymer with ionic side groups for the formation of a conjugated

T. T. Filate, Z. Genene, E. Wang
Department of Chemistry and Chemical Engineering
Chalmers University of Technology
Göteborg SE-412 96, Sweden
E-mail: ergang@chalmers.se
T. T. Filate, W. Mammo
Department of Chemistry
Addis Ababa University
PO Box 33658, Addis Ababa Ethiopia
E-mail: wendimagegn.mammo@aau.edu.et
S. Tang, L. Edman
The Organic Photonics and Electronic Group
Department of Physics, Umeå University
Umeå SE-901 87, Sweden
E-mail: ludvig.edman@umu.se
The ORCID identification number(s) for the author(s) of this article can be found under https://doi.org/10.1002/admt.202301696

DOI: 10.1002/admt.202301696

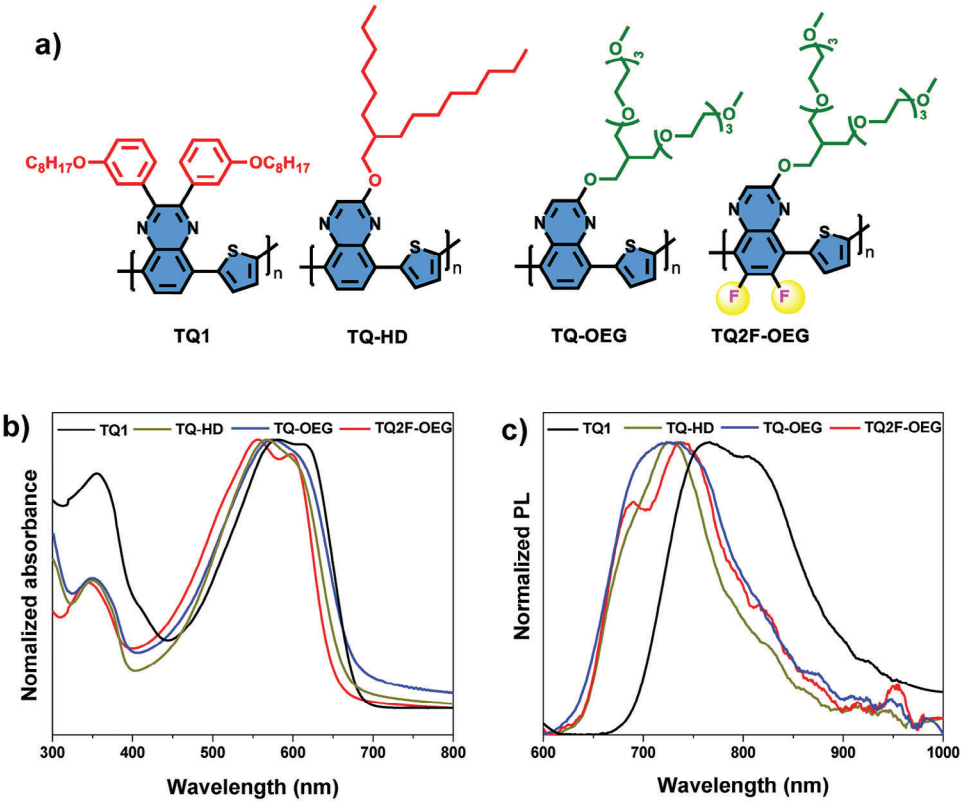

Figure 1. a) The chemical structures of the four polymers. b) The normalized absorption spectra and c) the normalized PL spectra of thin films of the four polymers, as identified in the insets. The thickness of the spin-coated thin films was 80 nm.

polyelectrolyte,[8] or chemically grafting different types of hydrophilic groups, such as oligo(ethylene glycols) (OEGs), onto the conjugated main chain.[9]

In order for conjugated polymers to become a good fit for high-volume applications, it is not only important to render their environmental footprint acceptable, but it is also critical that their synthesis can be scaled up at low cost. This is unfortunately not an easy task.[10] However, hydrophobic thiophene-quinoxaline (TQ) donor-acceptor conjugated polymers exhibit relatively low structural complexity, and they can therefore be synthesized at potentially low cost.[11] Specifically, the preparation of TQ-based polymers involves a few and high-yielding synthesis steps starting from commercially available materials and uncomplicated purification.

Here, we report on the pioneering design, synthesis and application of hydrophilic TQ-based conjugated polymers through the chemical modification of two "reference" TQ-based polymers: poly[2,3-bis-(3-octyloxyphenyl)quinoxaline-5,8-diyl-*alt*-thiophene-2,5-diyl] (**TQ1**) and poly[2-((2-hexyldecyl)oxy)quinoxaline-5,8-diyl-*alt*-thiophene-2,5-diyl] (**TQ-HD**) (**Figure 1**a). We specifically replace the two alkoxyphenyl groups of **TQ1** and the alkyloxy group of **TQ-HD** with a branched OEG chain, that is, 13-(methyleneoxy)−2,5,8,11,15,18,21,24-octaoxapentacosane, to prepare two new polymers, namely poly[2-((13-(2,5,8,11-tetraoxadodecyl)−2,5,8,11-tetraoxatetradecan-14-yl)oxy)quinoxaline-5,8-diyl-*alt*-thiophen-2,5-diyl] (**TQ-OEG**) and poly[6,7-difluoro-2-((13-(2,5,8,11-tetraoxadodecyl)−2,5,8,11-tetraoxatetradecan-14-yl)oxy)quinoxaline-5,8-diyl-*alt*-thiophen-2,5-diyl] (**TQ2F-OEG**) (Figure 1a). We call attention to that **TQ2F-OEG** comprises two fluorine atoms on the quinoxaline moiety. As desired, our modification procedure renders both **TQ-OEG** and **TQ2F-OEG** highly hydrophilic, as manifested by a high solubility of 35.7 and 43.5 mg mL^{-1} in a water:ethanol (15:85 V:V) blend solvent, respectively. We finally demonstrate the functionality of these new hydrophilic polymers by their successful introduction as the emitter in light-emitting electrochemical cells (LECs). The best-performing LEC device comprised a blend of the **TQ2F-OEG** emitter and a Li salt as the active material positioned between two air-stable electrodes, and it delivered deep-red emission with the emission peak at 670 nm and a radiance of 185 μW m^{-2} at a low drive voltage of 2.3 V.

2. Results and Discussion

TQ-based compounds have been reported and verified as comparatively low-cost and efficient conjugated polymers for optoelectronic application and this motivated our selection of the polymeric core structure.[12] Notably, the synthesis of TQ-based polymers commonly requires less than four synthetic steps, and the total reaction yield is relatively high, as manifested in reported total reaction yields of >62%.[11a,e] Rech *et al.*[13] also recently reported that the cost for the synthesis of a TQ-based conjugated polymer, for example, poly[6,7-difluoro-2-((2-hexyldecyl)oxy)quinoxaline-5,

8-diyl-*alt*-thiophene-2,5-diyl], can be as low as \$30.3 g^{-1}. We have also noted that the cost of the OEG-based polymer **TQ2F-OEG** is \$44.89 \$ g^{-1}.

Most conjugated polymers, including earlier TQ-based conjugated polymers, are endowed with hydrophobic substituents in order to render them soluble in, and processable from, non-polar solvents, but the herein desired solubility in polar solvents required the use of hydrophilic pendants. We specifically opted to graft hydrophilic ether-based side groups, in the form of branched OEG chains, onto the polymeric backbone. From a polar solubility perspective, we found in the literature that an ethylenedioxy-based side-chain is preferable over a methylenedioxy-based side chain despite the fact that the latter features a higher oxygen atom content. In this context, we note that Woutersen *et al.*[14] reported that the ethylenedioxy group exhibits a comparatively higher partial charge on the oxygen atom than the methylenedioxy group.

Figure 1a presents the molecular structures of the four investigated TQ-based donor-acceptor conjugated polymers. **TQ1** and **TQ-HD** are the two hydrophobic "reference polymers", which feature two alkoxyphenyl solubilizing side groups and one alkyloxy side group, respectively. **TQ-OEG** shares the same conjugated core structure, but it is instead endowed with branched OEG solubilizing side chains that comprise, on average, six ethyleneoxide units per conjugated polymer repeating unit. **TQ2F-OEG** is further distinguished by the presence of two fluorine atoms on the quinoxaline moiety.

Details on the synthesis of the monomers and polymers can be found in the supporting information and **Scheme** S1 (Supporting Information) summarizes the different synthetic steps of **TQ-HD**, **TQ-OEG**, and **TQ2F-OEG**. In brief, the key alkylation step in the synthesis of monomer **7c** of **TQ-HD** was conducted through the Mitsunobu reaction between 2-hexyldecanol and compound **6a** in the presence of triphenylphosphine (PPh_3) and diisopropyl azodicarboxylate (DIAD).[13] The specific OEG-functionalized alkylating reagent **3** was prepared in two steps, starting from 3-chloro-2-(chloromethyl)prop-1-ene (**1**) and 2-(2-(2-methoxyethoxy)ethoxy)ethan-1-ol. Intermediate compound **2** was converted to **3** using a hydroboration-oxidation sequence, as depicted in **Scheme** S1 (Supporting Information). The Mitsunobu reaction between alcohols **6a** or **6b** and compound **3** was used to prepare key monomers **7a** and **7b**, required for the synthesis of **TQ-OEG** and **TQ2F-OEG**, respectively. Note that the Mitsunobu reaction, instead of the usual Williamson ether synthesis, was selected for the introduction of the side chains, in order to avoid the extra synthetic steps required to prepare alkyl halides.

The polymer synthesis was achieved by the Stille polymerization reaction between the respective dibromo monomer and 2,5-bis(trimethylstannyl)thiophene, using a palladium catalyst. **TQ-OEG** and **TQ2F-OEG** were precipitated from a non-polar solvent (hexanes (60+% *n*-hexane)) because they, in contrast to the hydrophobic reference polymers, are (slightly) soluble in methanol. Methanol was still used in the Soxhlet extraction to remove the oligomeric chains from **TQ-OEG** and **TQ2F-OEG**. We mention that it was not possible to purify **TQ-OEG** and **TQ2F-OEG** by column chromatography over silica gel because of their high affinity for the polar stationary phase. The chemical structures of **TQ-OEG** and **TQ2F-OEG** were confirmed by ^{1}H NMR spectroscopy (Figure S1, Supporting Information).

The molecular weights and polydispersity indices of **TQ1**, **TQ-HD**, and **TQ2F-OEG** were established to be 24.0 kDa/2.6, 15.4 kDa/3.4, and 16.0 kDa/2.2, respectively, with the aid of gel permeation chromatography (GPC). Figure S2 (Supporting Information) presents the thermogravimetric analysis traces of **TQ-HD**, **TQ-OEG**, and **TQ2F-OEG**. The onset for thermal degradation is ranging between 300 °C for **TQ1**[11a] to 382 °C for **TQ-HD**, which implies that all four polymers will be robust towards thermal degradation induced by self-heating at a high current density in light-emitting devices.[15]

The solubility of the polymers was first investigated by computing their three Hansen solubility parameters (HSPs), i.e., the molecular dispersion (δ_D), the dipole (δ_P) and the hydrogen bonding (δ_H), using the so-called Hoftyzer–Van Krevelen group contribution method.[16] The HSPs were calculated with **Equations** S1–S3 (Supporting Information), using the tabulated parameter values in Tables S1–S4 (Supporting Information). The capacity of a solvent to dissolve a solute, here the polymer, is indicated by the interaction radius (R_a), that is, the effective distance between the solvent and the solute in Hansen space:

$$R_a = \left(4\left(\delta_{D1} - \delta_{D2}\right)^2 + \left(\delta_{P1} - \delta_{P2}\right)^2 + \left(\delta_{H1} - \delta_{H2}\right)^2\right)^{1/2} \quad (1)$$

The smaller the value of R_a, the higher is the dissolution capacity of the solvent for the solute. The HSPs of the water:ethanol solvent blend at different compositions, and the HSPs of the four TQ-based polymers, are presented in Table S5 and S6 (Supporting Information), respectively. Figure S3 and Table S7 (Supporting Information) reveal that **TQ-OEG** and **TQ2F-OEG**, in combination with the water:ethanol solvent blend, feature much lower R_a values than **TQ1** and **TQ-HD**, which implies that the former two polymers should exhibit a correspondingly higher solubility in the water: ethanol solvent blend.

We note in passing that You *et al.*[9e] have determined experimental HSPs for a polymer (PTQ-6bO2) with a similar structure to that of **TQ2F-OEG** using the multiple solvent method. We therefore computed the R_a values using their experimental HSPs to determine the solubility of PTQ-6bO2 in the water: ethanol solvent system, and found that a high solubility should be possible in this solvent system, when water is the major component.

Table S8 (Supporting Information) presents an experimental solubility study, which confirms that **TQ-OEG** and **TQ2F-OEG**, but not **TQ1** and **TQ-HD**, indeed are highly soluble in the hydrophilic water:ethanol solvent blend system, for a water:ethanol (V:V) concentration ranging from 50:50 to 5:95. Interestingly, we find that **TQ-OEG** and **TQ2F-OEG** are effectively insoluble in both neat water and neat ethanol (Table S8, Supporting Information), and that all four polymers are soluble in common non-polar solvents, such as chloroform and toluene. The former can be explained by that solvent self-association effects commonly are strong in neat solvents, which limit the solubilizing interactions between the solute and the solvent. When a second solvent is added to the solvent system, this self-association can be disrupted, and the interactions with the solute increase.[17] Nevertheless, the achieved good solubility of the **TQ-OEG** and **TQ2F-OEG** polymers in the water:ethanol solvent blends shows that our design motif has been fulfilled. Moreover, the fact that these two hydrophilic polymers feature very poor solubility in neat water

and water-dominant water:ethanol solvent blends is actually an advantage during the disposal of waste contaminated with these polymers, since they can be precipitated out in water-dominant environments and easily removed.

Figure 1b presents the UV–vis absorption spectra of spin-coated thin films of the neat polymers, whereas the corresponding spectra in dilute chloroform solution are displayed in Figure S4 (Supporting Information). All four polymers exhibit broad absorption bands covering essentially the entire visible region, with the main film absorption peak (from high to low energy) being positioned at 556 nm for **TQ2F-OEG**, 568 nm for **TQ-HD**, 575 nm for **TQ-OEG**, and 582 nm for **TQ1**. The red-shifted absorption of **TQ1** can be explained by the extended conjugation induced by its two phenyl rings (see Figure 1a). A comparison between Figure 1c and Figure S4 (Supporting Information) shows that the absorption in the neat film is red-shifted compared to the dilute chloroform solution, and that this red shift is much larger for the two OEG-containing polymers (>50 nm) than **TQ-HD** (13 nm) and **TQ1** (1 nm). Table S9 (Supporting Information) informs that the absorption onset for the solid thin films varies between 674 and 704 nm, and that the corresponding optical energy gap ranges between 1.83 and 1.91 eV.

Figure 1c presents the photoluminescence (PL) spectra of spin-coated neat films of the four polymers, whereas Figure S5 (Supporting Information) presents the same data for the polymers in a dilute solution. Table S9 (Supporting Information) summarizes the key data of the PL measurements and also presents the values for the PL quantum yield (PLQY). The four neat polymer films emit primarily in the near-infrared regime, that is, above 700 nm, and it is notable that the red shift in going from dilute solution to neat film is rather large at 48–70 nm, which indicates that aggregation effects are prominent in the neat films. This conclusion is supported by the observation that the PLQY also drops significantly in going from dilute solution to neat film, particularly for **TQ-HD** and **TQ-OEG**.

Cyclic voltammetry (CV) was employed to establish the capacity of the four polymers for electrochemical p-type and n-type doping, and to derive the values for their highest occupied molecular orbital (HOMO), lowest unoccupied molecular orbital (LUMO), and the electrochemical energy gap (E_g^{EC}). Figure S6 (Supporting Information) shows that all four polymers feature reversible oxidation and reduction reactions in cyclic voltammetry, which implies capacity for electrochemical p-type and n-type doping, respectively.[18] We find that the electrochemical energy gap is slightly larger than the optical energy gap, and that the HOMO and LUMO energy levels of the **TQ1** polymer are deeper than those of the other three polymers.

With the opportunity for processing from a benign solvent mixture and the capacity for bipolar electrochemical doping established, we turn to the investigation of the merit of **TQ-OEG** and **TQ2F-OEG** in LEC devices. The active material of an LEC comprises an emissive semiconductor, for example, a conjugated polymer, and mobile ions. The mobile ions redistribute during the initial LEC operation to first form injection-facilitating electric double layers (EDLs) at the electrode interfaces, and thereafter to enable for electrochemical doping of the semiconductor by functioning as charge-compensating counterions.[19] For the hydrophobic **TQ-HD** and **TQ1**, the mobile ions were introduced by dissolving a $LiCF_3SO_3$ salt in a hydroxyl-capped trimethylolpropane ethoxylate (TMPE-OH) compound.[20] In the case of the hydrophilic **TQ-OEG** and **TQ2F-OEG**, the $LiCF_3SO_3$ salt could be directly dissolved into mobile ions by the hydrophilic polymer, which eliminates the need for a separate ion-dissolving compound, for example, TMPE-OH. The active-material ink solvent was THF for the two hydrophobic polymers and a water:ethanol (15:85 V:V) solvent blend for the two hydrophilic polymers. The LEC devices were fabricated by spin-coating a thin film of the active-material ink on top of an indium-tin-oxide/poly(3,4-ethylenedioxythiophene) polystyrene sulfonate (ITO/PEDOT:PSS) anode, and thereafter depositing an air-stable Al cathode by thermal evaporation.

Figures 2a–c and Figure S8 (Supporting Information) present the temporal evolution of the radiance (left y-axis) and the drive voltage (right y-axis) for pristine LEC devices with the emissive copolymer being **TQ-HD** (Figure 2a), **TQ-OEG** (Figure 2b), **TQ2F-OEG** (Figure 2c) and **TQ1** (Figure S8, Supporting Information). The pristine LEC devices were driven by a constant current density of either 250 or 1000 mA cm^{-2}, as specified in the figure insets. We elected to measure and present the radiance, instead of the luminance, since the primary LEC emission is outside of the visible range.

All four LECs exhibit an increasing radiance and decreasing voltage with time during the initial operation, which is attributed to the initial mobile-ion-induced formation of the EDLs at the two electrode interfaces which enables for an increasingly balanced injection of electrons and holes and, consequently, a higher exciton formation rate. The lowering of the voltage during constant-current LEC operation is due to the increase in the effective conductance of the active material, which can be assigned to the ion-enabled electrochemical doping of the emissive copolymer.[21] The observed deviation from this behavior for the **TQ2F-OEG**-based LEC at longer times implies that a conductivity-damaging side reaction is ongoing in the active material in parallel with the electrochemical doping.[22]

Figure 2d displays the EL spectra of the LEC devices at a steady state. All four LECs exhibit a broad and relatively non-structured EL spectrum, with a full width at half maximum of 152, 97, 106, and 137 nm for **TQ1**, **TQ-HD**, **TQ-OEG,** and **TQ2F-OEG**, respectively. The EL peak is positioned at 675 nm for three of the LEC devices, with the exception being the hydrophobic **TQ1** LEC that features a significant ≈60 nm red shift of the entire EL envelope, as evidenced by the shift in the EL peak to 735 nm. A similar red shift was observed for the PL (Figure 1c), and it is attributed to the extended conjugation that results from the presence of two octyloxyphenyl rings on **TQ1** (see Figure 1a).

Table 1 presents a summary of key performance metrics of the four LEC devices. Interestingly, the best combined device performance was obtained with the LECs derived from the two hydrophilic polymers processed from the green solvent mixture (water:ethanol (15:85 V:V)). The **TQ-OEG** and **TQ2F-OEG** LECs exhibited the lowest drive voltage of 2.9 and 2.3 V, respectively, and the **TQ2F-OEG** LEC also delivered the highest radiance of 185 μW cm^{-2} and the largest external quantum efficiency (EQE) of 0.043%. The fact that the LEC based on the hydrophobic **TQ-HD** polymer featured a slightly higher radiance than the **TQ-OEG** LEC can be explained by the much higher PLQY of the former in the solid state (see Table S9, Supporting Information). The emission efficiency of the LEC fabricated from the hydrophobic

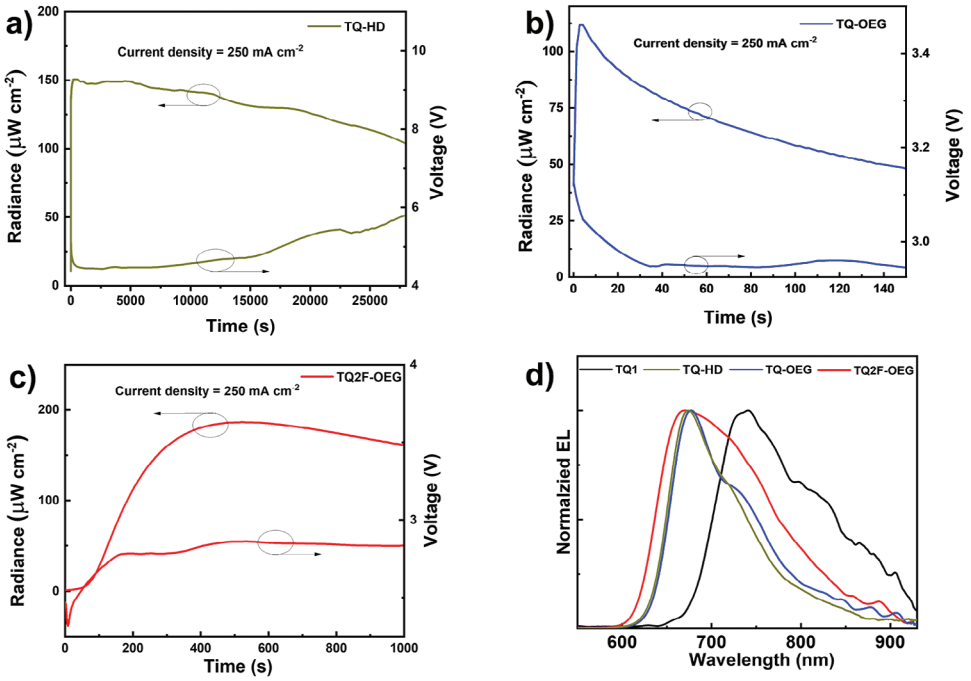

Figure 2. a–c) The temporal evolution of the radiance (left y-axis) and the voltage (right y-axis) of the LEC devices during driving with a constant current density of 250 mA cm^{-2}, with the emitting polymer being a) **TQ-HD**, b) **TQ-OEG** and c) **TQ2F-OEG**. d) The steady-state EL spectra of the four LEC devices, with the emitting polymer as identified in the inset.

TQ1 is more than 100 times lower than the other three LEC devices, despite that its active material featured the highest PLQY. It has been demonstrated that the ion mobility and electrochemical doping of LEC devices can be severely inhibited if the emissive semiconductor forms crystals.[23] Since it has been demonstrated that the **TQ1** copolymer has a strong propensity to form crystalline domains,[24] it appears plausible that this is the culprit that results in the poor performance of the **TQ1** LEC.

In the same context, it is interesting that the best LEC performance is attained with the fluorinated hydrophilic emitter **TQ2F-OEG**. Several preceding LEC studies have concluded that the introduction of fluorine atoms can result in efficient packing of the semiconductor units, which in turn inhibits the ion transport.[15c,25] However, it is plausible that the particular molecular structure of **TQ2F-OEG** results in an attractive compromise, where the flexible OEG groups provide for efficient ion transport, whereas the fluorine-induced conformational locking[26] enhances the stacking of the conjugated core units for efficient electron transport.[27] Regardless, an important lesson to be drawn from our study is that it is possible to obtain a similar, or even improved, LEC performance by endowing the semiconductor with OEG groups, which facilitates for an environmentally benign LEC fabrication.

From Figure 2a,c, we have noted that the alkylated polymer **TQ-HD** has shown better stability compared to OEG-based polymer **TQ-OEG** upon device operation. There are two plausible explanations for this stability difference. Firstly, unlike alkyl side chains, OEG groups have structures that are more flexible. This flexibility in the side chain results in more closely packed π-π stacking, which consequently reduces the ionization potential of OEG-based polymers.[27e,28] This low ionization potential makes OEG-based conjugated polymers vulnerable to irreversible oxidation under potential bias. The second plausible explanation may be the interaction of hydrophilic OEG polymers with ionic species. The performance of LECs is dependent on both ionic and electronic conductivity.[20] The hydrophilic nature of the OEG polymers promotes a large amount of ion infiltration inside the clusters of the conjugated polymer. This phenomenon could

Table 1. LEC performance as a function of the active material.

Active material	Current density [mA cm^{-2}]	EL peak [nm]	Turn on time [s][a)]	Peak radiance [μW cm^{-2}]	Voltage [V]	EQE [%]
TQ1:TMPE-OH:$LiCF_3SO_3$	1000	735	–	10	3.6	0.0006
TQ-HD:TMPE-OH:$LiCF_3SO_3$	250	675	2	150	5.5	0.036
TQ-OEG:$LiCF_3SO_3$	250	675	2	111	2.9	0.026
TQ2F-OEG:$LiCF_3SO_3$	250	670	124	185	2.3	0.043

[a)] radiance > 50 μW cm^{-2}

result in a gradual deterioration of the electronic conductivity of OEG-based polymers. On the other hand, in hydrophobic alkylated polymers, the pure conjugated polymer domains facilitate the electronic conductivity of the device.

Even though OEG-based emitters have the advantage of processing from environmentally benign solvents and eliminating the need for a third-party ion-solvating agent in the active layer, they suffer from poor device stability. For instance, the radiance of **TQ-OEG**-based device reached below 80% of the peak radiance within 25 s (Table S10, Supporting Information). We have extended the device test to observe the stability in the presence of an external ion-solvating agent. Figure S8 (Supporting Information) presents the temporal evolution of LEC device fabricated from **TQ-OEG**, TMPE-OH, and $LiCF_3SO_3$ as active layer blends in the mass ratio of 100:10:3. Interestingly, we have observed that the addition of the external ion-solvating additive significantly improved the LEC device stability. As summarized in Table S10 (Supporting Information), thepeak radiance degradation time to 80% (T_{80}) was extended to over 3200 s after the addition of an ion-solvating additive in the emissive layer. This may be attributed to the enhanced ion-solvating capability of the **TQ-OEG**:TMPE-OH blend.[29] This indicates that the OEG-based LEC devices have room for improvement by adding ion-solvating agents.

3. Conclusion

The health hazard and environmental footprint of the hydrophobic solvents commonly used during the printing and coating fabrication of organic electronic devices is a concerning issue. Here, we report on the design and synthesis of two hydrophilic emissive conjugated polymers, **TQ-OEG** and **TQ2F-OEG**, which were rendered hydrophilic through the grafting of polar OEG solubilizing groups onto a thiophene-quinoxaline conjugated core backbone and thereby can be processed from a green water:ethanol solvent mixture. We show that the introduction of the OEG groups also enables for a direct dissolution of salts by the neat polymer for the attainment of solid-state ion mobility without adding ion-dissolving compounds. We utilize these properties for the design and development of LECs, the active material of which can be solution cast from an environmentally benign water:ethanol-based ink. We specifically show that such a green-solvent-processed LEC device, comprising a blend of the **TQ2F-OEG** emitter and a Li salt as the active material positioned between two air-stabile electrodes, delivers deep-red emission (peak wavelength = 670 nm) with a radiance of 185 μW m^{-2} at a low drive voltage of 2.3 V.

Supporting Information

Supporting Information is available from the Wiley Online Library or from the author.

Acknowledgements

The authors thank the Swedish Research Council (2021-04778, 2019–02345 and 2018–07072), the Swedish Energy Agency (P2021-00032 and 50779-1), Bertil & Britt Svenssons stiftelse för belysningsteknik (2021 höst-14 and 2022 höst-31), the Knut and Alice Wallenberg Foundation (WISE-AP01-D02), and the Wallenberg Initiative Materials Science for Sustainability, WISE. for financial support. TTF and WM acknowledge financial support from the International Science Programme, Uppsala University, Sweden.

Conflict of Interest

The authors declare no conflict of interest.

Data Availability Statement

The data that support the findings of this study are available from the corresponding author upon reasonable request.

Keywords

aqueous-processable polymers, conjugated polymers, Hansen solubility parameters, light-emitting electrochemical cells, oligo(ethylene glycol)

Received: October 12, 2023
Published online:

[1] H. Bronstein, C. B. Nielsen, B. C. Schroeder, I. Mcculloch, *Nat. Rev. Chem.* **2020**, *4*, 66.
[2] a) M. A. M. Leenen, V. Arning, H. Thiem, J. Steiger, R. Anselmann, *Phys. Status Solidi A* **2009**, *206*, 588; b) Y. Lin, C. Cai, Y. Zhang, W. Zheng, J. Yang, E. Wang, L. Hou, *J. Mater. Chem. A* **2017**, *5*, 4093; c) A. Sandström, L. Edman, *Energy Technol.* **2015**, *3*, 329.
[3] C. Larsen, P. Lundberg, S. Tang, J. Ràfols-Ribé, A. Sandström, E. Mattias Lindh, J. Wang, L. Edman, *Nat. Commun.* **2021**, *12*, 4510.
[4] a) L. Bhatia, S. Johri, R. Ahmad, *AMB Express* **2012**, *2*, 65; b) C. Capello, U. Fischer, K. Hungerbühler, *Green Chem.* **2007**, *9*, 927.
[5] N. A. Mirgane, A. V. Karnik, *Green Chem. Lett. Rev.* **2011**, *4*, 269.
[6] C. M. Alder, J. D. Hayler, R. K. Henderson, A. M. Redman, L. Shukla, L. E. Shuster, H. F. Sneddon, *Green Chem.* **2016**, *18*, 3879.
[7] a) C. Ceriani, M. Scagliotti, T. Losi, A. Luzio, S. Mattiello, M. Sassi, N. Pianta, M. Rapisarda, L. Mariucci, M. Caironi, L. Beverina, *Adv. Electron. Mater.* **2023**, *9*, 2201160; b) F. De Lera-Garrido, A. Sánchez-Ruiz, J. Rodríguez-López, J. Tolosa, J. C. García-Martínez, *Dyes Pigm.* **2020**, *179*, 108410; c) M. Mooney, Y. Wang, A. Nyayachavadi, S. Zhang, X. Gu, S. Rondeau-Gagné, *ACS Appl. Mater. Interfaces* **2021**, *13*, 25175; d) P. Vahdatiyekta, M. Zniber, J. Bobacka, T.-P. Huynh, *Anal. Chim. Acta* **2022**, *1221*, 340114; e) B. Zhao, Z. Liang, Y. Zhang, Y. Sui, Y. Shi, X. Zhang, M. Li, Y. Deng, Y. Geng, *ACS Macro Lett.* **2021**, *10*, 419.
[8] a) M. R. Pinto, K. S. Schanze, *Synthesis* **2002**, *2002*, 1293; b) A. O. Patil, Y. Ikenoue, F. Wudl, A. J. Heeger, *J. Am. Chem. Soc.* **1987**, *109*, 1858; c) S. Shi, F. Wudl, *Macromolecules* **1990**, *23*, 2119; d) V. Cimrová, W. Schmidt, R. Rulkens, M. Schulze, W. Meyer, D. Neher, *Adv. Mater.* **1996**, *8*, 585; e) Y. Jin, G. C. Bazan, A. J. Heeger, J. Y. Kim, K. Lee, *Appl. Phys. Lett.* **2008**, *93*, 123304; f) S. Kee, M. A. Haque, Y. Lee, T. L. Nguyen, D. Rosas Villalva, J. Troughton, A.-H. Emwas, H. N. Alshareef, H. Y. Woo, D. Baran, *ACS Appl. Energy Mater.* **2020**, *3*, 8667; g) D. Vak, S.-H. Oh, D.-Y. Kim, *Appl. Phys. Lett.* **2009**, *94*, 243305; h) Z. Gu, Q.-D. Shen, J. Zhang, C.-Z. Yang, Y.-J. Bao, *J. Appl. Polym. Sci.* **2006**, *100*, 2930; i) A. Duarte, K.-Y. Pu, B. Liu, G. C. Bazan, *Chem. Mater.* **2011**, *23*, 501; j) L. Edman, M. Pauchard, B. Liu, G. Bazan, D. Moses, A. J. Heeger, *Appl. Phys. Lett.* **2003**, *82*, 3961.
[9] a) H.-H. Lu, Y.-S. Ma, N.-J. Yang, G.-H. Lin, Y.-C. Wu, S.-A. Chen, *J. Am. Chem. Soc.* **2011**, *133*, 9634; b) L. Shang, S. Qu, Y. Deng, Y. Gao, G. Yue, S. He, Z. Wang, Z. Wang, F. Tan, *J. Mater. Chem. C* **2022**, *10*, 506; c) C. Kim, H. Kang, N. Choi, S. Lee, Y. Kim, J. Kim, Z. Wu, H. Y.

Woo, B. J. Kim, *J. Mater. Chem. C* **2020**, *8*, 15224; d) S. Lee, Y. Kim, Z. Wu, C. Lee, S. J. Oh, N. T. Luan, J. Lee, D. Jeong, K. Zhang, F. Huang, T.-S. Kim, H. Y. Woo, B. J. Kim, *ACS Appl. Mater. Interfaces* **2019**, *11*, 45038. e) J. Neu, S. Samson, K. Ding, J. J. Rech, H. Ade, W. You, *Macromolecules* **2023**, *56*, 2092.

[10] R. Po, G. Bianchi, C. Carbonera, A. Pellegrino, *Macromolecules* **2015**, *48*, 453.

[11] a) E. Wang, L. Hou, Z. Wang, S. Hellström, F. Zhang, O. Inganäs, M. R. Andersson, *Adv. Mater.* **2010**, *22*, 5240; b) R. Singh, G. Pagona, V. G. Gregoriou, N. Tagmatarchis, D. Toliopoulos, Y. Han, Z. Fei, A. Katsouras, A. Avgeropoulos, T. D. Anthopoulos, M. Heeney, P. E. Keivanidis, C. L. Chochos, *Polym. Chem.* **2015**, *6*, 3098; c) Y. Wu, Y. Zheng, H. Yang, C. Sun, Y. Dong, C. Cui, H. Yan, Y. Li, *Sci. China Chem.* **2020**, *63*, 265; d) W. Zhuang, H. Zhen, R. Kroon, Z. Tang, S. Hellström, L. Hou, E. Wang, D. Gedefaw, O. Inganäs, F. Zhang, M. R. Andersson, *J. Mater. Chem. A* **2013**, *1*, 13422; e) C. Sun, F. Pan, H. Bin, J. Zhang, L. Xue, B. Qiu, Z. Wei, Z.-G. Zhang, Y. Li, *Nat. Commun.* **2018**, *9*, 743.

[12] a) G. K. Dutta, T. Kim, H. Choi, J. Lee, D. S. Kim, J. Y. Kim, C. Yang, *Polym. Chem.* **2014**, *5*, 2540; b) D. Yuan, F. Pan, L. Zhang, H. Jiang, M. Chen, W. Tang, G. Qin, Y. Cao, J. Chen, *Sol. RRL* **2020**, *4*, 2000062.

[13] J. J. Rech, J. Neu, Y. Qin, S. Samson, J. Shanahan, R. F. Josey, H. Ade, W. You, *ChemSusChem* **2021**, *14*, 3561.

[14] B. Ensing, A. Tiwari, M. Tros, J. Hunger, S. R. Domingos, C. Pérez, G. Smits, M. Bonn, D. Bonn, S. Woutersen, *Nat. Commun.* **2019**, *10*, 2893.

[15] a) E. Fresta, J. Dosso, J. Cabanillas-Gonzalez, D. Bonifazi, R. D. Costa, *ACS Appl. Mater. Interfaces* **2020**, *12*, 28426; b) J. Ràfols-Ribé, N. D. Robinson, C. Larsen, S. Tang, M. Top, A. Sandström, L. Edman, *Adv. Funct. Mater.* **2020**, *30*, 1908649; c) S. Tang, P. Murto, X. Xu, C. Larsen, E. Wang, L. Edman, *Chem. Mater.* **2017**, *29*, 7750.

[16] a) D. W. Van Krevelen, K. T. Nijenhuis, in *Properties of Polymers*, (4th Ed.) (Eds.: D. W. Van Krevelen, K. T. Nijenhuis), Elsevier, Amsterdam **2009**, pp. 189–227; b) C. Lee, H. R. Lee, J. Choi, Y. Kim, T. L. Nguyen, W. Lee, B. Gautam, X. Liu, K. Zhang, F. Huang, J. H. Oh, H. Y. Woo, B. J. Kim, *Adv. Energy Mater.* **2018**, *8*, 1802674.

[17] a) I. A. Finneran, P. B. Carroll, M. A. Allodi, G. A. Blake, *Phys. Chem. Chem. Phys.* **2015**, *17*, 24210; b) S. Alavi, S. Takeya, R. Ohmura, T. K. Woo, J. A. Ripmeester, *J. Chem. Phys.* **2010**, *133*, 074505; c) V. Amenta, J. L. Cook, C. A. Hunter, C. M. R. Low, H. Sun, J. G. Vinter, *J. Am. Chem. Soc.* **2013**, *135*, 12091.

[18] S. Tang, H. A. Buchholz, L. Edman, *J. Mater. Chem. C* **2015**, *3*, 8114.

[19] J. F. Fang, Y. L. Yang, L. Edman, *Appl. Phys. Lett.* **2008**, *93*, 063503.

[20] J. Ràfols-Ribé, X. Zhang, C. Larsen, P. Lundberg, E. M. Lindh, C. T. Mai, J. Mindemark, E. Gracia-Espino, L. Edman, *Adv. Mater.* **2022**, *34*, 2107849.

[21] P. Matyba, K. Maturova, M. Kemerink, N. D. Robinson, L. Edman, *Nat. Mater.* **2009**, *8*, 672.

[22] J. Fang, P. Matyba, N. D. Robinson, L. Edman, *J. Am. Chem. Soc.* **2008**, *130*, 4562.

[23] a) S. Tang, C. Larsen, J. Ràfols-Ribé, J. Wang, L. Edman, *Adv. Opt. Mater.* **2021**, *9*, 2002105; b) L. Edman, M. Pauchard, D. Moses, A. J. Heeger, *J. Appl. Phys.* **2004**, *95*, 4357.

[24] a) D. Täuber, W. Cai, O. Inganäs, I. G. Scheblykin, *ACS Omega* **2017**, *2*, 32; b) T. Yamamoto, B.-L. Lee, H. Kokubo, H. Kishida, K. Hirota, T. Wakabayashi, H. Okamoto, *Macromol. Rapid Commun.* **2003**, *24*, 440; c) E. Wang, J. Bergqvist, K. Vandewal, Z. Ma, L. Hou, A. Lundin, S. Himmelberger, A. Salleo, C. Müller, O. Inganäs, F. Zhang, M. R. Andersson, *Adv. Energy Mater.* **2013**, *3*, 806.

[25] a) C. Zhang, R. Liu, D. Zhang, L. Duan, *Adv. Funct. Mater.* **2020**, *30*, 1907156; b) M. Mone, S. Tang, P. Murto, B. A. Abdulahi, C. Larsen, J. Wang, W. Mammo, L. Edman, E. Wang, *Chem. Mater.* **2019**, *31*, 9721; c) D. Tordera, J. J. Serrano-Pérez, A. Pertegás, E. Ortí, H. J. Bolink, E. Baranoff, M. K. Nazeeruddin, J. Frey, *Chem. Mater.* **2013**, *25*, 3391; d) A. F. Henwood, E. Zysman-Colman, *Top. Curr. Chem.* **2016**, *374*, 36; e) M. S. Lowry, J. I. Goldsmith, J. D. Slinker, R. Rohl, R. A. Pascal, G. G. Malliaras, S. Bernhard, *Chem. Mater.* **2005**, *17*, 5712.

[26] a) Y. Liu, Z. Zhang, S. Feng, M. Li, L. Wu, R. Hou, X. Xu, X. Chen, Z. Bo, *J. Am. Chem. Soc.* **2017**, *139*, 3356; b) T. Lei, X. Xia, J.-Y. Wang, C.-J. Liu, J. Pei, *J. Am. Chem. Soc.* **2014**, *136*, 2135.

[27] a) X.-Y. Wang, Y. Liu, Z.-Y. Wang, Y. Lu, Z.-F. Yao, Y.-F. Ding, Z.-D. Yu, J.-Y. Wang, J. Pei, *J. Polym. Sci.* **2022**, *60*, 538; b) P. A. Finn, I. E. Jacobs, J. Armitage, R. Wu, B. D. Paulsen, M. Freeley, M. Palma, J. Rivnay, H. Sirringhaus, C. B. Nielsen, *J. Mater. Chem. C* **2020**, *8*, 16216; c) D. Ohayon, A. Savva, W. Du, B. D. Paulsen, I. Uguz, R. S. Ashraf, J. Rivnay, I. Mcculloch, S. Inal, *ACS Appl. Mater. Interfaces* **2021**, *13*, 4253; d) I. P. Maria, B. D. Paulsen, A. Savva, D. Ohayon, R. Wu, R. Hallani, A. Basu, W. Du, T. D. Anthopoulos, S. Inal, J. Rivnay, I. Mcculloch, A. Giovannitti, *Adv. Funct. Mater.* **2021**, *31*, 2008718; e) B. Meng, H. Song, X. Chen, Z. Xie, J. Liu, L. Wang, *Macromolecules* **2015**, *48*, 4357; f) H.-C. Yen, Y.-C. Lin, W.-C. Chen, *Macromolecules* **2021**, *54*, 1665.

[28] G. Krauss, F. Meichsner, A. Hochgesang, J. Mohanraj, S. Salehi, P. Schmode, M. Thelakkat, *Adv. Funct. Mater.* **2021**, *31*, 2010048;

[29] Q. Sun, Y. Li, Q. Pei, *J. Disp. Technol.* **2007**, *3*, 211.